



Innovative thermoplastic chitosan obtained by thermo-mechanical mixing with polyol plasticizers



Marie Matet^a, Marie-Claude Heuzey^{a,*}, Eric Pollet^b, Abdellah Ajji^a, Luc Avérous^b

^a CREPEC, Department of Chemical Engineering, Polytechnique Montreal, P.O. Box 6079, Station Centre-Ville, Montreal, Quebec, Canada H3C 3A7

^b BioTeam/ICPEES-ECPM, UMR, Université de Strasbourg, 25 rue Becquerel, 67087 Strasbourg Cedex 2, France

ARTICLE INFO

Article history:

Received 25 January 2013

Accepted 26 February 2013

Available online 5 March 2013

Keywords:

Chitosan

Polyol

Plasticization

Thermo-mechanical treatment

Morphology

Properties

ABSTRACT

Chitosan shows a degradation temperature lower than its melting point, which prevents its development in several applications. One way to overcome this issue is the plasticization of the carbohydrate. In this work plasticized chitosan was prepared by a thermo-mechanical kneading approach. The effects of different non-volatile polyol plasticizers (glycerol, xylitol and sorbitol) were investigated. The microstructure and morphology were determined using FTIR, XRD, TEM and SEM in order to understand the plasticization mechanism. Sorbitol, which is the highest molecular weight polyol used, resulted in plasticized chitosan with the highest thermal, mechanical and rheological properties. On the other hand, the sample plasticized with glycerol, the lowest molecular weight polyol, had the most important amorphous phase content and the lowest thermal, mechanical and rheological properties. Also, when the polyol content increased in the formulation, the plasticized chitosan was more amorphous and consequently its processability easier, while its properties decreased.

© 2013 Elsevier Ltd. All rights reserved.

1. Introduction

Chitin is the most abundant polysaccharide on earth after cellulose. Chitin is a biopolymer present, for instance, in the cell wall of fungi or in the shell of arthropods such as crustaceans (e.g., crabs, shrimps or lobsters). Chitosan is the most important chitin derivative. Chitosan is obtained through the controlled deacetylation of chitin in the presence of NaOH (Domard & Rinaudo, 1983; Ravi Kumar, 2000; Rinaudo, 2006; Roberts, 1992). It is mainly a linear polymer of β -(1-4)-linked D-glucosamine (deacetylated unit) and N-acetyl-D-glucosamine (acetylated unit). In the last few decades, chitosan has become a particularly interesting biomaterial because of its antimicrobial properties, biocompatibility and biodegradability. Chitosan can be used in many areas such as biomedical, cosmetology, waste water treatment, agriculture and food industry (Ravi Kumar, 2000; Rinaudo, 2006). In biomedical and biopharmaceutical applications, chitosan can be used for the development of controlled release drug delivery systems and for its wound healing properties, and its efficiency against bacteria and viruses (Ilium, 1998). In the food industry, chitosan has been utilized in different shapes and for different applications. For example, it has been used for food coatings or edible films to improve food conservation (Dutta, Tripathi, Mehrotra, & Dutta, 2009; Kittur,

Kumar, & Tharanathan, 1998; Shahidi, Arachchi, & Jeon, 1999). Chitosan-based films may prevent bacteria development on food surfaces because of its antibacterial and antifungal activities. Its efficiency has been shown to be a function of the degree of deacetylation (DDA) and molecular weight (No, Young Park, Ho Lee, & Meyers, 2002; Takahashi, Imai, Suzuki, & Sawai, 2008), the process used to fabricate the films (Li, Zivanovic, Davidson, & Kit, 2011; Zivanovic, Li, Davidson, & Kit, 2008), the shape (nanobeads, microspheres, fibers...) (Kong et al., 2008; Qi, Xu, Jiang, Hu, & Zou, 2004; Sadeghi et al., 2008), the acid used for dissolution (Pillai, Paul, & Sharma, 2009), and the presence of essential oils (Zivanovic, Chi, & Draughon, 2005) or metal ions (Chen, Wu, & Zeng, 2005; Wang, Du, & Liu, 2004).

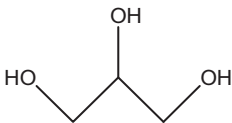
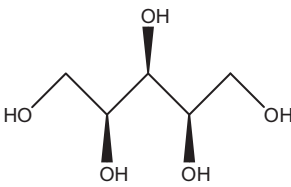
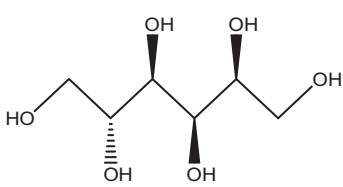
Solvent casting is a conventional method to produce chitosan-based films. Chitosan, at low concentration, is dissolved in acidic conditions (generally in acetic acid solutions), and the mixture is then cast in a Petri dish at moderate temperature (from ambient to 50 °C) until complete solvent evaporation (Dutta et al., 2009; Yi et al., 2005). Chitosan films produced with the solvent casting method are fragile at small thicknesses; for larger thicknesses, the internal tension increases and a rough surface is obtained (Balau, Lisa, Popa, Tura, & Melnig, 2004).

Since it is difficult to scale-up the solvent casting method to obtain chitosan-based films, and because the properties of these films are not robust enough for a large range of applications, chitosan transformation using a conventional melt processing approach would be a highly desirable alternative. For instance, films could be industrially produced at large scale in a continuous

* Corresponding author at: 2500 chemin de Polytechnique, Montreal, Quebec, Canada H3T 1J4. Tel.: +1 514 340 4711x5930; fax: +1 514 340 4159.

E-mail address: marie-claude.heuzey@polymtl.ca (M.-C. Heuzey).

Table 1
Main characteristics of the polyols used.

	Glycerol	Xylitol	Sorbitol
Chemical structure			
State (at ambient temperature)	Liquid	Powder	Powder
Melting point (°C)	20	94	95
Boiling point (°C)	182	216	296
Molar mass (g/mol)	92.1	152.2	182.2
Number of OH group/molecule	3	5	6

process, such as extrusion. This technique is a priori not applicable because neat chitosan degrades before it melts. A new and interesting approach has been proposed recently, inspired by the works developed around the plasticization of starch (Avérous & Halley, 2009). This new technique involves the thermo-mechanical treatment of chitosan in the presence of non-volatile plasticizer (glycerol) (Epure, Griffon, Pollet, & Avérous, 2011). A diluted acid solution (acetic acid), which acts as a de-structuring agent, is added to the system. The different components, chitosan, glycerol and acetic acid solutions were “paste”-blended in a batch mixer for 15 min at a set temperature of 80 °C with a rotor speed of 100 rpm. Glycerol-plasticized chitosan films were obtained after compression molding. The advantage of this approach is that the plasticized chitosan can further be melt-blended or coated as a thermoplastic in order to obtain a thermoplastic-like film with antibacterial and antifungal properties, which can be used for packaging or hygiene applications.

The first papers on plasticized starch, the so-called “thermoplastic starch,” have been published at the end of the eighties (Avérous, 2004). With several hundreds of publications, this topic presents now a strong background. Several polyols with different chemical structures are typically used for starch plasticization. Sorbitol, xylitol and maltitol have higher molecular weight than glycerol. It was shown that when a polyol with higher molecular weight was used, the tensile strength and the modulus increased, the thermal stability was better and the phase transition temperature of the starch increased (Li & Huneault, 2011; Qiao, Tang, & Sun, 2011). Also when the polyol content in the multiphase systems increased, those properties were affected in the same way, except for tensile strength and modulus that decreased (Li & Huneault, 2011; Qiao et al., 2011; Van Soest & Knooren, 1997).

Different plasticizers (glycerol, sorbitol, sucrose and polyethylene glycol) were also tested with chitosan processed by the solvent casting method (Arvanitoyannis, Kolokuris, Nakayama, Yamamoto, & Aiba, 1997; Quijada-Garrido, Laterza, Mazón-Arechederra, & Barrales-Rienda, 2006; Rotta & Ozório, 2009; Srinivasa, Ramesh,

& Tharanathan, 2007). The tensile strength and modulus decreased when the polyol content increased, whereas elongation at break increased in the presence of a polyol. In addition, CO₂ and water vapour permeability decreased when glycerol was added but increased with sorbitol addition (Arvanitoyannis et al., 1997; Srinivasa et al., 2007). However, as far as plasticized chitosan prepared by a thermo-mechanical process is concerned, only glycerol has been studied so far, as a non-volatile plasticizer.

The present study is based on the plasticization of chitosan by a thermo-mechanical treatment using various polyol contents, types and polyol mixtures. The aim of the study is to analyze the relationships between formulations, microstructure – morphology and properties (thermal, rheological and mechanical) of different plasticized chitosans. The aging of the samples is also monitored through the evolution of the rheological properties. The main goal is to open a wide range of new applications for chitosan, through the development of innovative materials by controlling the different steps of elaboration (formulation, process).

2. Materials and methods

2.1. Materials

Chitosan (ChitoClear®) was purchased from Primex (Iceland). Its degree of deacetylation (DDA) is 96% and its weight-average molecular weight is in the range of 250–300 kDa. It contains a 0.1 % ash residue.

The polyols used in this work (glycerol, xylitol, and sorbitol) are presented in Table 1. The polyols and glacial acetic acid were purchased from Sigma-Aldrich and used as received.

2.2. Sample preparation

An acetic acid solution at 3%, v/v was first prepared with glacial acetic acid and deionised water. For the unplasticized formulation, the acetic acid solution was slowly added to the chitosan

Table 2
Formulations and nomenclature of chitosan systems.

Sample	Acetic acid (3% v/v)/chitosan (wt%/wt%)	Chitosan/glycerol (wt%/wt%)	Chitosan/xylitol (wt%/wt%)	Chitosan/sorbitol (wt%/wt%)
ChiA	75/25			
ChiAG10	75/25	91/9		
ChiAG25	75/25	80/20		
ChiAG50	75/25	67/33		
ChiAX10	75/25		91/9	
ChiAX50	75/25		67/33	
ChiAS10	75/25			91/9
ChiAS50	75/25			67/33
ChiAG25X25	75/25	67/16.5	67/16.5	
ChiAG25S25	75/25	67/16.5		67/16.5
ChiAX25S25	75/25		67/16.5	67/16.5

powder and manually mixed to obtain pastes with a good homogeneity. For the plasticized formulation, the chosen polyol was first added dropwise to the chitosan powder. Then, the acetic acid solution was slowly added and manually mixed. The chitosan/acetic acid aqueous solution ratio was kept constant for all the pastes at 25/75 (wt/wt). Subsequently, the pastes were “melt” blended in an internal mixer Haake Rheocord 900 (Germany) at a set temperature of 80 °C for 15 min with a constant speed of 100 rpm of the roller blades rotor. This type of mixer provides a combination of elongational flow, laminar shear and distributive mixing (Manas-Zloczomer & Tadmor, 2009). The thermal probe reported a temperature of 95 °C in the mixing chamber, hence of the order of the melting points of xylitol and sorbitol (Table 1).

Finally, the pastes obtained at the end of the mixing process were hot press-molded at 110 °C for 15 min under a pressure of 270 bar to obtain sheets and films. Cooling to room temperature was achieved in 5 min under the same pressure. The sheet thickness was 1 mm for the mechanical and rheological tests and for the scanning electron microscopy (SEM) observations. The films

thickness was 80 μm for Fourier-transform infrared spectroscopy (FTIR) and X-ray diffraction (XRD).

The different formulations are summarized in Table 2 with the corresponding nomenclatures. Different contents were set for the polyols (three for glycerol, two for xylitol and sorbitol): 10, 25 or 50 wt% of the chitosan content. The prepared films and sheets were kept in a desiccator at room temperature (24 °C). Addition of toluene in the desiccator atmosphere prevented fungus development.

2.3. Characterization techniques

2.3.1. Fourier transform infrared spectroscopy (FTIR)

A Perkin Elmer 65 FT-IR (USA) was used to record the infrared spectra. IR spectra were collected with a resolution of 4 cm^{-1} using an accumulation of 32 scans in a wavenumber range of 650–4000 cm^{-1} . The 80 μm thickness films were directly tested at room temperature in horizontal attenuated total reflectance (ATR) mode.

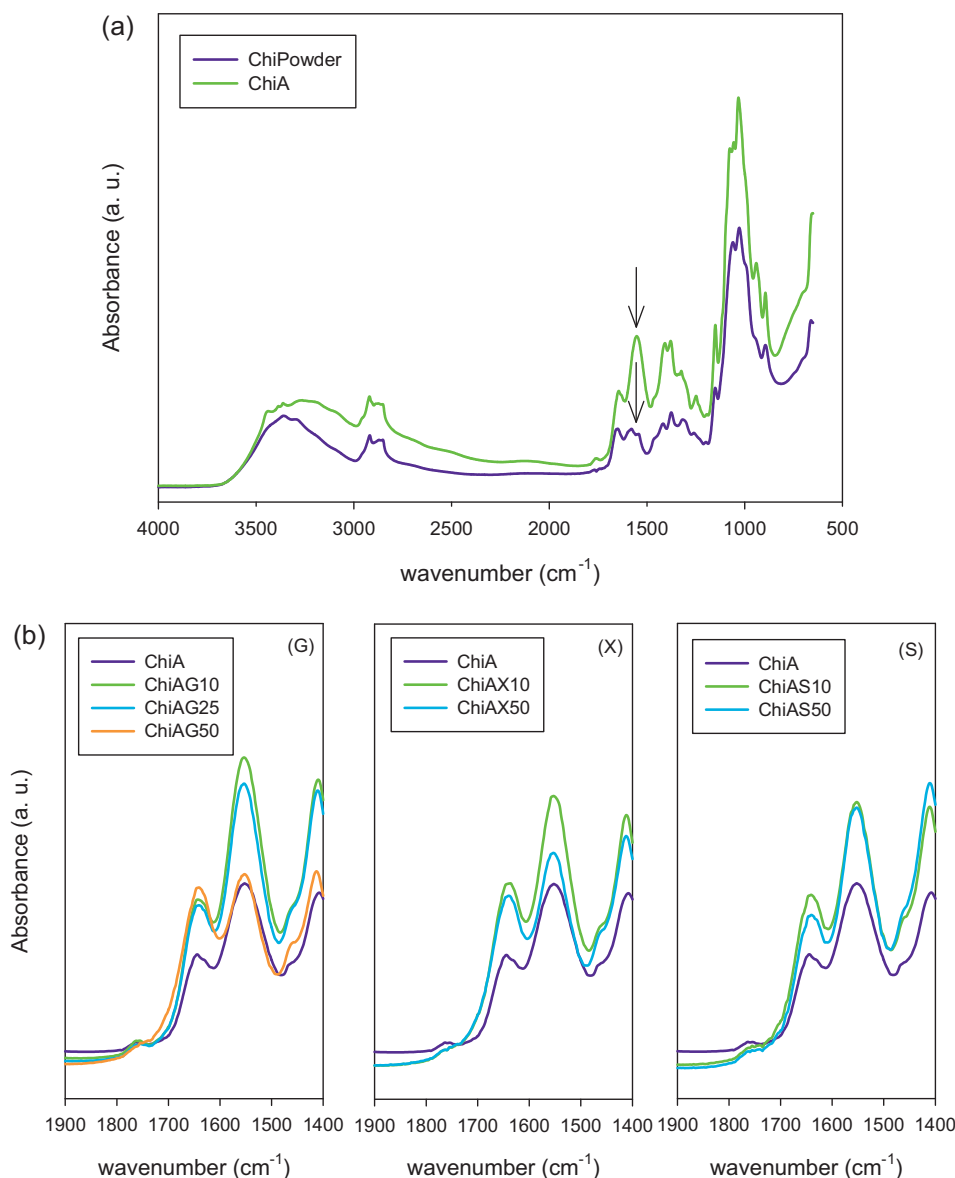


Fig. 1. FTIR spectra. (a) comparison of chitosan powder and sample ChiA. The N–H peak at 1578 cm^{-1} is shown by the arrows, (b) effect of polyol type and content: (G) glycerol, (X) xylitol and (S) sorbitol.

2.3.2. X-ray diffraction (XRD)

To investigate the crystallinity and structuration of the materials, X-ray diffraction spectra were obtained at room temperature with a powder diffractometer Philips X'PERT (Netherlands) equipped with a monochromatic Cu K α (1.5418 Å) X-ray source. The voltage used was 50 kV. The angle range was scanned from 5° to 35° with a step size 0.02° and a scanning time of 2 s by step.

2.3.3. Microscopy

2.3.3.1. Transmission electron microscopy (TEM). TEM images of the chitosan powder were obtained using a JEOL JEM-2100F (Japan) microscope operating at a 200 kV accelerating voltage. A small quantity of the powder was dispersed in pure water with ultrasonication for 20 min. Subsequently, some particles were disposed on a TEM grid and the water evaporated.

2.3.3.2. Scanning electron microscopy (SEM). A high resolution Hitachi S-4700 (Japan) microscope operated at 2 kV accelerating voltage was employed for field emission gun-SEM (FEG-SEM). The samples surfaces were cut using an ultramicrotome equipped with a diamond knife at –100 °C, and then coated with platinum vapor. The final observation area was approximately 200 μm \times 200 μm .

2.3.4. Thermogravimetric analysis (TGA)

The thermal degradation was determined by a TA Instruments Q 500 (USA). The temperature scans were performed from room temperature to 800 °C, with a heating rate of 10 °C/min under a nitrogen atmosphere. Each sample tested was less than 4 mg.

2.3.5. Rheological tests

Rheological properties were measured at 25 °C with a rheometer operated in strain-controlled (MCR 501, Anton Paar, Germany). A parallel disk flow geometry with a rough surface (25 mm diameter) was used. Rheological properties were monitored right after compression molding, and after 7, 14 and 21 days to analyze the impact of storage time.

2.3.6. Uniaxial tensile tests

Tensile tests were performed on an Instron E3000 (USA). The samples were rectangular plates (25 mm \times 50 mm \times 1 mm) and the tests were carried out at ambient temperature with a constant deformation rate of 50 mm/min. Stress-strain properties (tensile strength and elongation at break) were determined from the average of five measurements. To take into account the post processing aging and to test stabilized materials, the samples had been stored 3 weeks prior to the tests, as recommended by a previous study (Epure et al., 2011).

3. Results and discussion

3.1. Microstructure

3.1.1. Fourier transform infrared spectroscopy (FTIR)

In order to understand the interactions of the acetic acid solution and the various polyols with chitosan, FTIR spectroscopy was performed on chitosan powder and on the different samples. According to the literature, the FTIR-ATR spectrum of neat chitosan shows several typical bands: the stretching vibration of O–H group at 3400 cm^{-1} and the stretching vibration of N–H at 3280 cm^{-1} form a wide absorption band with a minimum at 3360 cm^{-1} ; the symmetric and anti-symmetric vibrations of CH_2 are located at 2918, 2865, 1415 and 1257 cm^{-1} ; the stretching vibration of the carbonyl group (C=O) in amide I has an absorption band at 1653 cm^{-1} , the bending absorption band of N=H in amide II appears at 1578 cm^{-1} and the stretching of C–N in amide III has

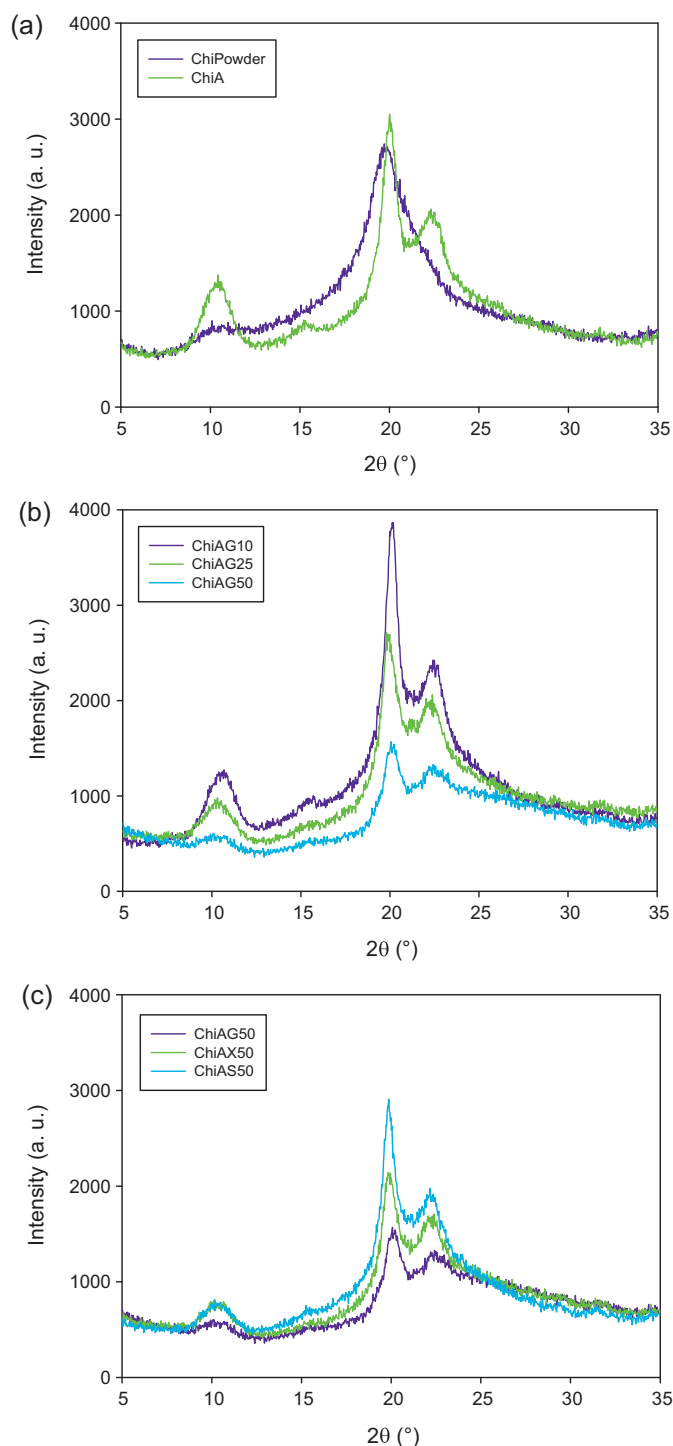


Fig. 2. X-ray diffraction patterns. (a) Comparison of chitosan powder and ChiA, (b) effect of glycerol content, (c) effect of different polyols (constant polyol concentration).

an absorption at 1376 cm^{-1} . Finally a small shoulder at 1541 cm^{-1} is attributed to the ammonium (NH_3^+) obtained by protonation of the amine group in acidic condition, and the stretching of C–O has a peak absorption at 1032 cm^{-1} (Brugnerotto et al., 2001; Lavorgna, Piscitelli, Mangiacapra, & Buonocore, 2010; Osman & Arof, 2003; Rivero, García, & Pinotti, 2010).

Fig. 1 presents the FTIR-ATR spectra for chitosan powder, unplasticized chitosan (ChiA) and different plasticized chitosans. The FTIR-ATR spectra of chitosan powder and ChiA (chitosan and acetic acid) are compared in Fig. 1a. ChiA shows the same FTIR

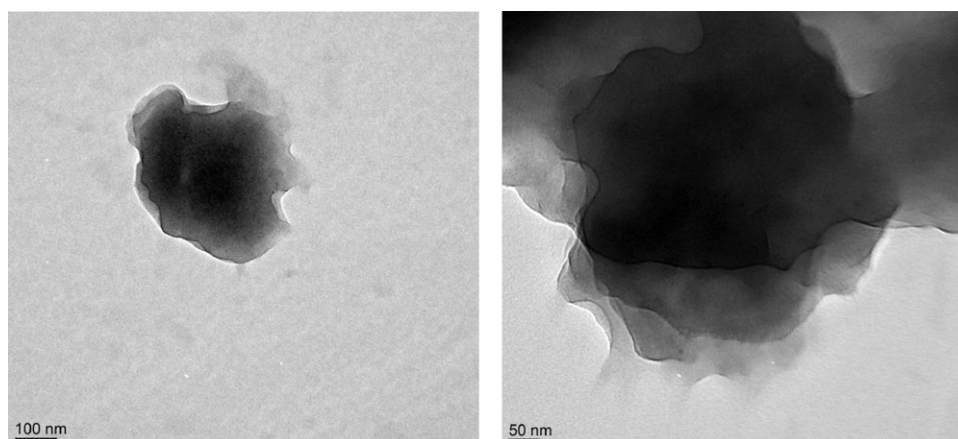


Fig. 3. TEM images of a chitosan powder particle.

spectrum shape than the chitosan powder, but with a higher intensity of the absorption bands. Because of the interaction between the —COO^- in acetic acid and the NH_3^+ in chitosan that results in the $\text{O}=\text{C}\text{—NHR}$ band, the small shoulder at 1541 cm^{-1} appears in the spectrum of ChiA, while the peak of the $\text{N}\text{—H}$ band at 1578 cm^{-1} present for chitosan powder disappears in the spectrum of ChiA, and the carbonyl band shifts from 1653 to 1644 cm^{-1} .

Fig. 1b presents the FTIR spectra of the plasticized chitosan samples between 1400 and 1900 cm^{-1} . When a polyol is added to chitosan with acetic acid, the $\text{C}=\text{O}$ absorption band at 1653 cm^{-1} and the $\text{N}\text{—H}$ absorption band at 1578 cm^{-1} are still present. Whatever the polyol, the $\text{N}\text{—H}$ absorption band appears at the same wavenumber and the $\text{C}=\text{O}$ absorption band in amide I shifts to a lower wavenumber (1644 cm^{-1} for ChiA and 1638 cm^{-1} for ChiAX50), when the polyol content increases. This shift to a lower wavenumber on the FTIR spectra indicates that the polyols interact with chitosan, and the hydrogen bonds formed in ChiA between acetic acid and the amide groups of chitosan (Fig. 1a) are replaced by

the interactions between the polyols and chitosan in the plasticized samples.

For each mixture added (results not shown), the same effects are observed, for each mixture added, the absorbance increase, and the $\text{C}=\text{O}$ and $\text{N}\text{—H}$ bands absorption shift to a lower wavenumber (respectively 1644 and 1554 cm^{-1} for ChiA, and 1638 and 1550 cm^{-1} for the samples with polyol mixture). In conclusion, all the polyols mixtures display interactions with chitosan, but FTIR is not a discriminatory technique to show differences between the different polyol mixture compositions.

3.1.2. X-ray diffraction (XRD)

Fig. 2 presents the X-ray diffraction patterns of various chitosan samples. The X-ray diffraction patterns of chitosan powder and ChiA are compared in Fig. 2a. Chitosan powder X-ray diffraction shows the presence of crystalline regions with two main peaks at 10.1° and 19.7° attributed to the $(0\ 2\ 0)$ and $(1\ 0\ 0)$ planes, respectively (Kittur, Vishu Kumar, & Tharanathan, 2003). The

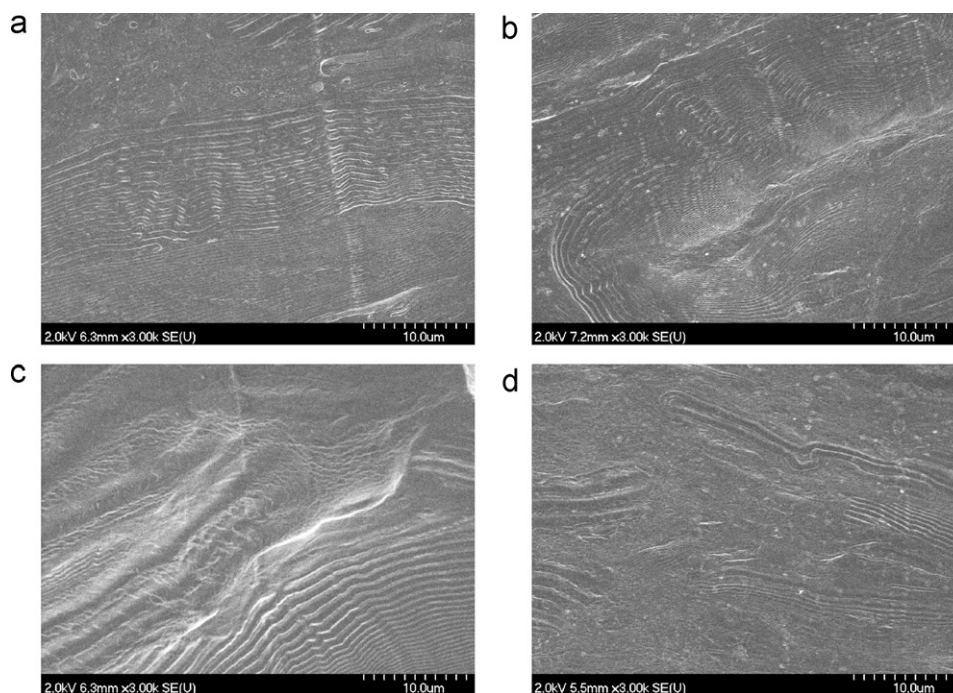


Fig. 4. SEM micrographs of four different samples. (a) ChiA, (b) ChiAG50, (c) ChiAX50 and (d) ChiAS50.

sample without polyol, ChiA, exhibits three different peaks related to the crystalline structure at 10.4° , 20.0° and 22.3° attributed to the (020), (100) and (110) planes, respectively (Kittur et al., 2003). Those peaks are narrower than the ones obtained for neat chitosan, and that may be explained by the different forms used for the analysis, i.e. powder for neat chitosan and pressed sheet for ChiA. The (020) reflection around 10° represents the acetamido groups which have the opportunity to create bonds with hydrogen, so that water molecules can be easily integrated to form hydrated crystals (Epure et al., 2011; Kittur et al., 2003).

The peaks around 20° and 22° are assigned to the crystal lattice of chitosan; it has been reported that chitosan crystallizes in an orthorhombic unit cell (Okuyama, Noguchi, Miyazawa, Yui, & Ogawa, 1997). For ChiA, the intensity of these peaks is higher than for neat chitosan powder, due to hydrogen bonding or different packing arrangement of the chains. The peaks are also detected at a higher reflection angle; according to Bragg's law, the spacing between the planes in a crystal lattice is inversely proportional to the angle of incidence. Hence the sample ChiA has a larger d -spacing that involves smaller unit cell dimensions.

The X-ray diffraction patterns on Fig. 2b and c of the different plasticized samples were obtained with the same amount of chitosan to compare them in a quantitative way. Fig. 2b shows the X-ray diffraction patterns of the glycerol-plasticized samples ChiAG10, ChiAG25 and ChiAG50 in order to demonstrate the effect of polyol content on the plasticized chitosan crystallinity. For the different contents of polyol in the sample, the three same peaks appear but, as the content of polyol increases in the sample, the peaks intensity decreases. Fig. 2a illustrates this behavior for glycerol, but the same trend was observed with xylitol and sorbitol. Hence the crystallinity of plasticized chitosan decreases with increasing content of polyol in the formulation.

In Fig. 2b, the effect of polyol type is examined. For a given plasticizer content, the crystallinity varies between the polyols. Sorbitol results in the highest crystallinity, while glycerol gives the lowest. Thus, it seems that glycerol shows the highest plasticizing efficiency. A possible explanation for this is that, since sorbitol and xylitol are solid at room temperature, they may recrystallize upon cooling and hence be less effective for chitosan plasticization than glycerol. This effect has also been observed for plasticized starch films (Talja, Helén, Roos, & Jouppila, 2007; Thirathumthavorn & Charoenrein, 2007). XRD spectra for xylitol and sorbitol were examined separately (results not shown) and compared with those of the plasticized chitosan formulations. The characteristic peaks of these neat polyols are not detected in the plasticized formulations (Fig. 2b), however most of these peaks overlap with those of chitosan, hence it is difficult to confirm or rule out the recrystallization of xylitol and sorbitol.

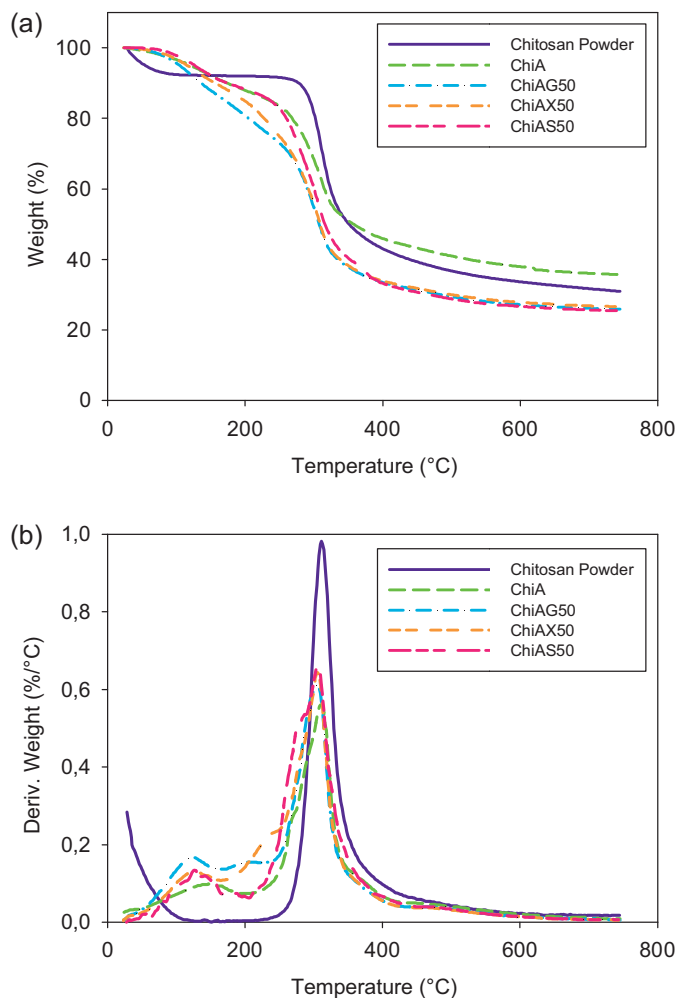


Fig. 5. TG (top) and DTG (bottom) curves of chitosan powder, chitosan plasticized with the three different polyols and the unplasticized sample ChiA.

3.2. Microscopy observations

3.2.1. Transmission electron microscopy (TEM)

In order to understand the effect of the plasticization mechanism, it is useful to examine the structure of the chitosan powder before dissolution in the acetic acid solution and before the thermo-mechanical treatment. To this end, some particles of chitosan powder were dispersed in water using ultrasonication and observed in transmission electronic microscopy.

Table 3
Characteristic degradation temperatures of unplasticized chitosan and the different plasticized chitosans.

Sample	$T_{98\%}$ ($^\circ\text{C}$)	$T_{50\%}$ ($^\circ\text{C}$)	1st stage T_{dmax1} ($^\circ\text{C}$)	Weight (%)	2nd stage T_{dmax2} ($^\circ\text{C}$)	Weight (%)
Chitosan powder	36	351	–	–	311	71
ChiA	79	355	138	93	312	62
ChiAG10	85	340	142	93	310	62
ChiAG25	72	315	123	92	307	55
ChiAG50	76	308	118	93	306	51
ChiAX10	97	346	142	94	310	63
ChiAX50	84	309	126	94	306	52
ChiAS10	100	346	144	94	311	62
ChiAS50	96	316	127	95	305	57
ChiAG25X25	81	308	140	91	306	51
ChiAG25S25	86	311	120	94	306	53
ChiAX25S25	100	315	131	95	306	56

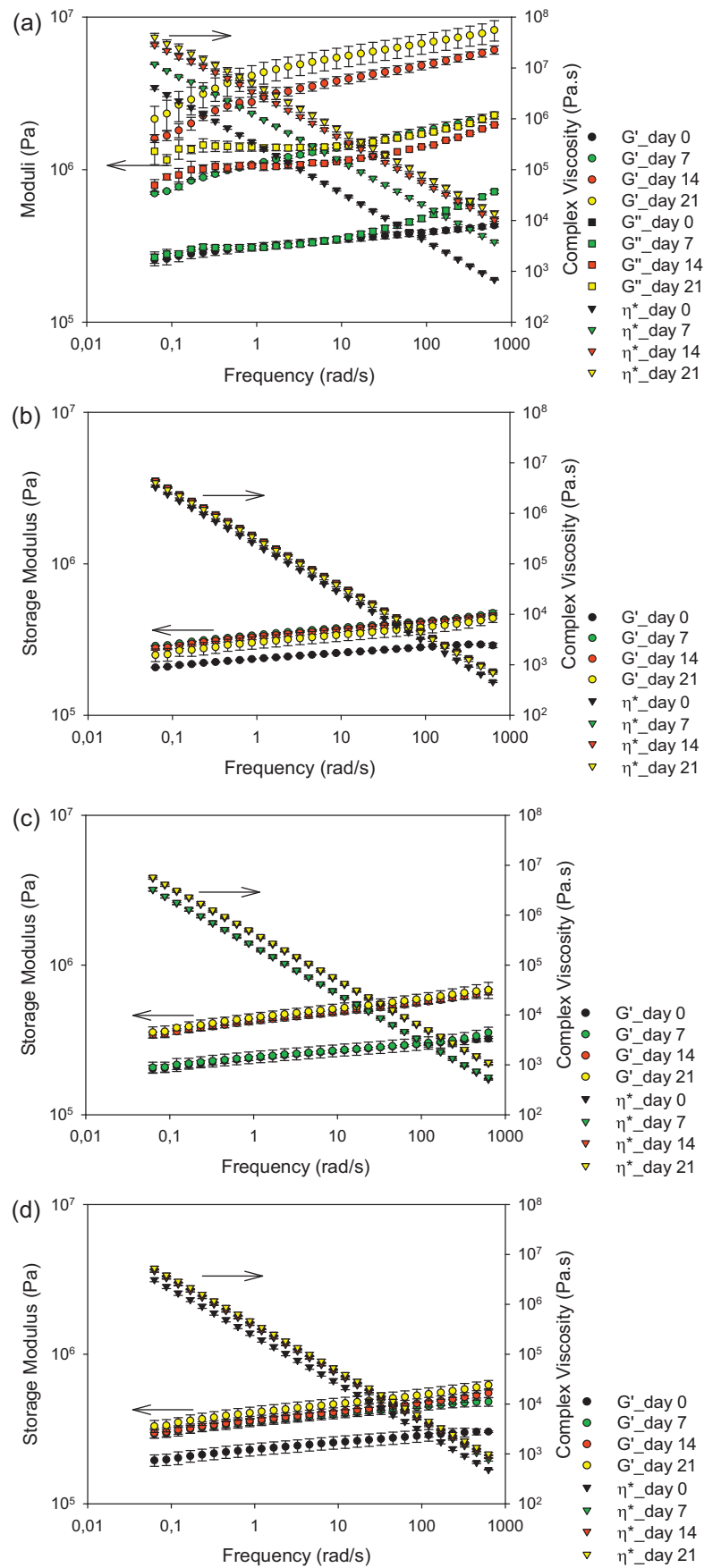


Fig. 6. Dynamic rheological properties of different samples. (a) ChiA, (b) ChiAG50, (c) ChiAX50 and (d) ChiAS50. Tests were performed at 25 °C under a strain of 0.001.

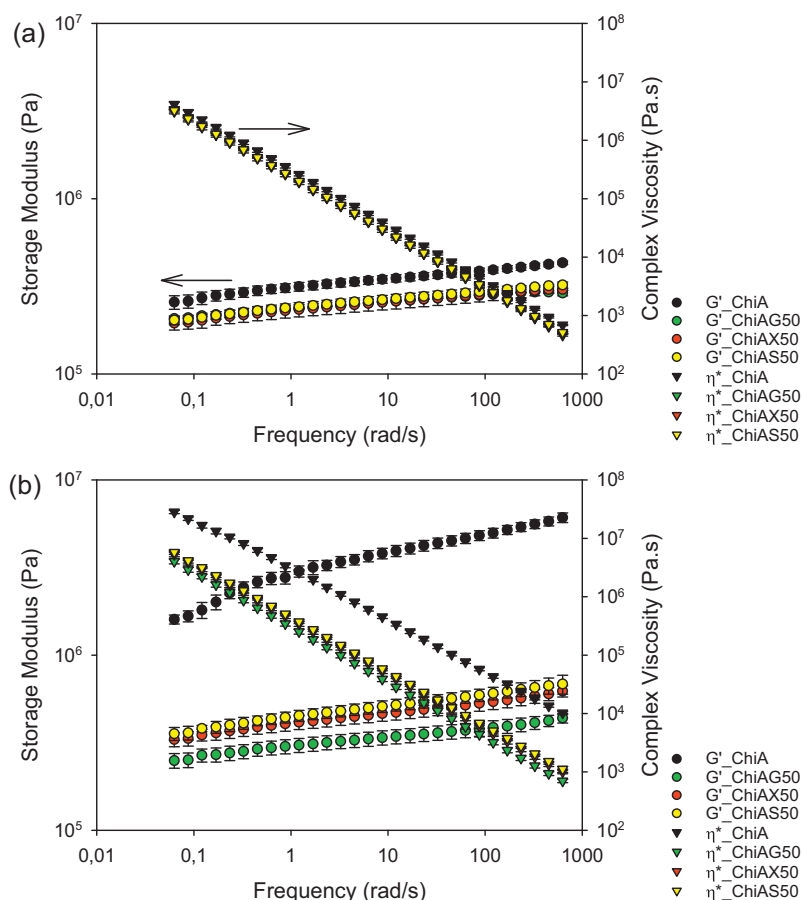


Fig. 7. Rheological properties for different samples tested on day 0 (a) and day 21 (b) after compression molding. Tests were performed at 25 °C under a strain of 0.001.

Fig. 3 shows an isolated chitosan powder particle at two different magnifications. The higher magnification allows observing that a chitosan powder particle consists of a stack of sheets, i.e. somehow similar to a layered structure. This supports the ordered structure detected in XRD and described in the literature (Okuyama et al., 1997).

3.2.2. Scanning electron microscopy (SEM)

Formulated samples (ChiA, ChiAG50, ChiAS50 and ChiAX50) were examined using SEM. The corresponding micrographs are presented in Fig. 4. For all the samples, a layered structure embedded in an amorphous “matrix” is observed. This microstructure is in agreement with the TEM images of the chitosan powder (Fig. 3), however it is much coarser and apparently observed from a different perspective. These micrographs are also in accordance with the XRD results, i.e. unplasticized and plasticized chitosan exhibit a certain degree of crystallinity. It seems that all the chitosan particles could not be entirely dissolved in the acetic acid solution, most probably because of the high chitosan to acetic acid solution ratio used (25/75 wt/wt), and despite the thermo-mechanical treatment applied to the chitosan particles. In the solvent casting method, the chitosan/acetic acid solution ratio commonly used is much lower, i.e., typically 4/96 wt/wt (Mucha, 1998). Conversely, the 25/75 ratio chosen in this study was aimed at obtaining an initial paste-like texture that could support the thermo-mechanical treatment in the batch mixer. Hence it is possible that not all the chitosan particles are completely dissolved, protonated and destructured in the plasticized formulations.

As for the amorphous “matrix” that hosts the chitosan particles, some differences are noticed between the samples with and

without polyol. In the overall surface area observed, the density of the layered structure decreases in the presence of the plasticizers, indicating nevertheless their “destructuring” effect. No obvious differences can be noticed between the three polyols.

3.3. Thermogravimetric analysis (TGA)

Thermogravimetric analysis was performed to assess the thermal stability of the various chitosan formulations. Fig. 5 shows the thermal degradation, in nitrogen atmosphere, of chitosan powder and different samples with and without polyol. Fig. 5a presents the relative weight loss (TG curves), while Fig. 5b shows the weight loss first derivative (DTG curves), as functions of temperature. The characteristic temperatures are reported in Table 3. From the curves one can see that unplasticized and plasticized chitosan decompose in two stages, the first weight loss stage shows water evaporation while the second stage corresponds to the thermal degradation of the samples. The maximum temperatures in the DTG curves for the two stages are reported in Table 3 as T_{dmax1} and T_{dmax2} , with the corresponding weights.

The chitosan powder shows a progressive weight loss (less than 10%) up to 120 °C due to water evaporation, while the thermal degradation starts around 310 °C. In agreement with previous work (Martino, Pollet, & Avérous, 2011), plasticized chitosan demonstrates a faster thermal degradation than unplasticized chitosan (ChiA). When the polyol content increases, the thermal degradation is also faster considering the lower T_{dmax} values for the first stage and the lower $T_{50\%}$ listed in Table 3. If we examine the $T_{50\%}$ values, chitosan plasticized with sorbitol is the formulation that results in the slowest thermal degradation, as may be expected from its

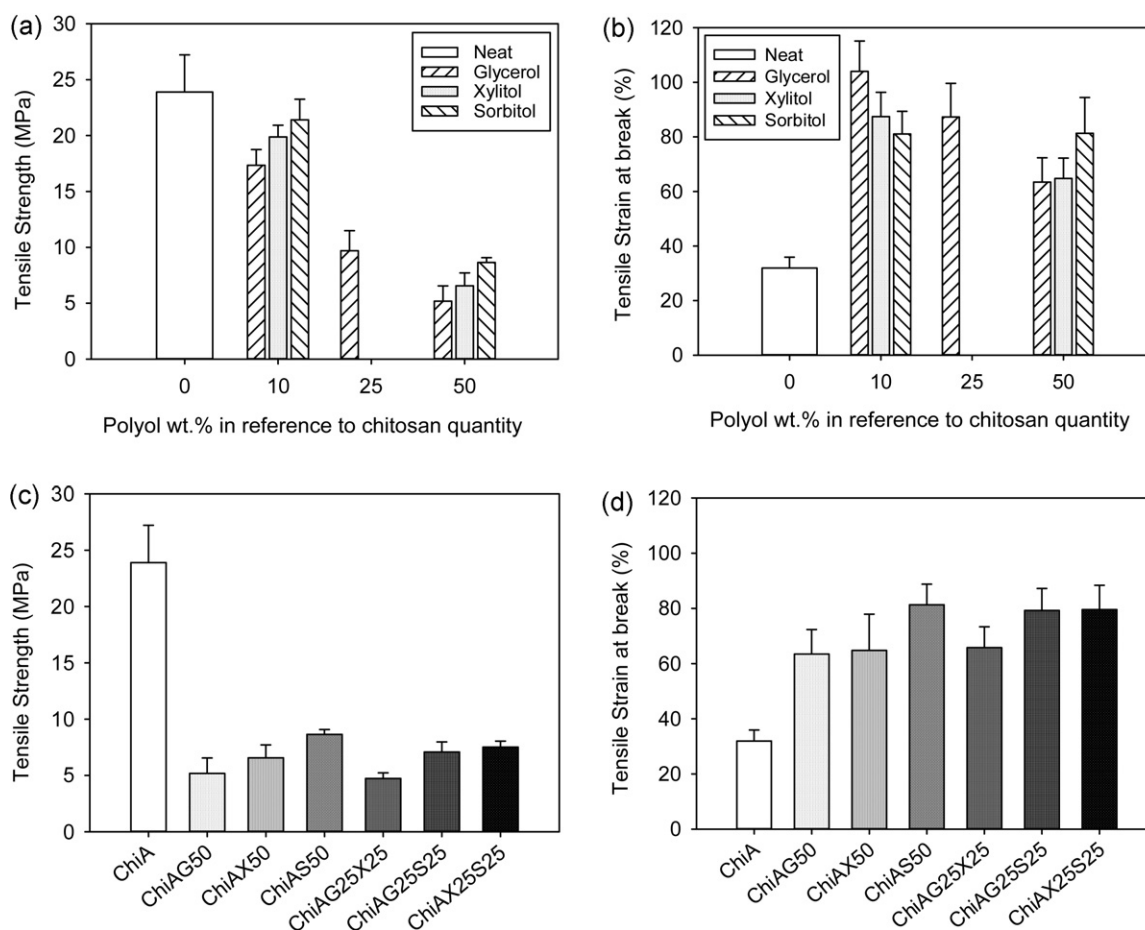


Fig. 8. Tensile strength (a and c) and tensile strain at break (b and d) for plasticized chitosan with different polyols and polyol contents.

characteristic temperatures (melting point and boiling point, Table 1). The T_{dmax} for the first stage shows the same trend (i.e. sorbitol is more stable), however the difference in the T_{dmax} values for the second stage is not significant. The weight loss for the 1st stage (water evaporation) is not significantly different for the various samples, as expected.

For the 2nd stage, a less important weight loss is observed for the chitosan powder in comparison with plasticized and unplasticized chitosan. In addition, for the 2nd stage the weight loss is almost the same for ChiA and chitosan plasticized with the lowest amount of polyol, regardless of the polyol type. However when the polyol content increases in plasticized chitosan, the weight loss recorded is larger for the 2nd stage, most probably due to polyol degradation.

Due to the respective compositions of the four samples, less residues remain at 800 °C for the plasticized samples as compared to ChiA. It is more likely that the polyol and remaining acetic acid solution are fully vaporized below 250 °C and only chitosan can leave residues.

Hence, thermal degradation is accelerated in the presence of polyols. However since sorbitol follows the same behavior as ChiA until 250 °C, it seems a better candidate in terms of thermal resistance in comparison with the others polyols.

3.4. Rheological tests

Monitoring of the rheological properties at room temperature as function of time may be indicative of the storage stability of these plasticized chitosan samples. Fig. 6 shows the elastic modulus and the complex viscosity as functions of frequency at 25 °C for four different samples: ChiA, ChiAG50, ChiAX50 and ChiAS50. These

results were obtained right after compression-molding (day 0) and for three different storage times: day 7, 14 and 21.

First, it can be observed that the complex viscosity is strongly shear-dependent, with a well-developed power-law behavior. There is no indication of a Newtonian plateau in any case. Second, the elastic modulus is higher than the loss modulus (shown here only for ChiA (Fig. 6a) for sake of clarity and conciseness), and both increase with shear rate. Hence the plasticized chitosan exhibits a solid-like behavior, similarly to plasticized starch (Valle, Buleon, Carreau, Lavoie, & Vergnes, 1998).

Fig. 6 shows that the rheological properties of the samples increase with storage time, most probably because of water (and acetic acid) evaporation. For example, at a frequency of 628 rad/s the ChiA complex viscosity on day 21 is multiplied by 15 with respect to day 0, for ChiAG50 by 1.5, and for ChiAX50 and ChiAS50 by 2. The increases are slightly lower at low frequencies. This storage stability variation is also similar to that observed for plasticized starch and has been investigated widely (Forsell, Hulleman, Myllärinen, Moates, & Parker, 1999; Van Soest, Hulleman, De Wit, & Vliegthart, 1996).

The rheological properties are seen to increase steadily with time for ChiA and ChiAG50 samples, however, the most significant increase occurs after day 7 for ChiAX50 and just after day 14 for ChiAS50. This can be due to the fact that sorbitol is the plasticizer with the highest concentration in –OH groups and glycerol the lowest. These hydroxyl groups can participate in the formation of a hydrogen bond network, with the participation of water molecules. This network can be more or less dense with the lowest density being expected for glycerol. Hence, water evaporation is faster in the case of glycerol than for xylitol and sorbitol. This means that

chitosan plasticized with sorbitol can retain the same rheological properties longer than chitosan plasticized with glycerol or xylitol.

Fig. 7 compares the complex viscosity and the storage modulus as functions of frequency for samples with and without polyol, and for day 0 and 21, after compression molding.

On day 0, the complex viscosities are almost the same for the four samples. However, the storage modulus of ChiA is 40% higher than that of the samples plasticized with a polyol. Hence the rheological properties presented in Fig. 7a show that the polyol type has no influence right after compression molding.

At day 21 (Fig. 7b), the differences are more noticeable between the sample without polyol and those with the different polyols used. ChiA exhibits a storage modulus 12 times higher than ChiAG50, 9 times higher than ChiAX50 and 8 times higher than ChiAS50.

The rheological properties also depend on the polyol choice: glycerol results in lower storage modulus while sorbitol in the highest. These results are in accordance with the XRD results: indeed, the samples with glycerol show the lowest crystallinity whereas those with sorbitol show the highest. This also confirms the better plasticizing efficiency of glycerol compared to the other polyols.

3.5. Uniaxial tensile tests

The effects of polyol type, content and mixture on the mechanical properties of plasticized chitosan are shown in Fig. 8.

The unplasticized chitosan (ChiA) has the highest tensile strength (Fig. 8a). Also, the higher the polyol content is, the larger is the decrease in tensile strength with respect to ChiA. For sorbitol, a decrease of 13% is observed when the chitosan and sorbitol ratio is 91/9 wt/wt, and of 67% when the ratio is 67/33 wt/wt. Glycerol, alone (Fig. 8a) or mixed with another polyol (Fig. 8c), is the plasticizer that results in the lowest tensile strength, whatever the content. On the contrary, sorbitol gives the highest tensile strength at low and high content, either alone or in polyols mixture. Those results are in agreement with the rheological properties and the XRD results, and may again be explained by a possible recrystallization of sorbitol at room temperature.

Tensile strain at break (Fig. 8b) increases when the polyol content is 10%, as expected, but when it is too high (25 and 50%) the tensile strain at break decreases again, except for sorbitol, whose quantity seems not to influence this property. For the higher content of polyol in plasticized chitosan, sorbitol results in the highest value of the strain at break, while glycerol and xylitol are very similar with low strain at break values. In the case of polyol mixtures, the total quantity of polyol is the same than in ChiAG50, iChiAX50 or ChiAS50, and the tensile strain at break is also higher than for ChiA. The glycerol/xylitol blend (ChiAG25X25) gives a lower value than the two mixtures that contain sorbitol (ChiAG25S25 and ChiAX25S25), as shown in Fig. 8d. Hence polyols play an important role in chitosan plasticization, however excessive polyol content may cancel out this effect on the tensile strain at break. We speculate that for the highest content of polyol, a phase separation may occur and reduce the plasticization efficiency; however, this hypothesis would require further investigation.

4. Conclusions

Different innovative multiphase systems based on plasticized chitosan obtained by thermo-mechanical treatment in the presence of acetic acid solution and polyols were elaborated and fully studied in this work. The effects of three different polyols (glycerol, xylitol and sorbitol) on various properties of plasticized chitosan were examined and compared to those of unplasticized chitosan. FTIR spectra confirmed the interaction between chitosan and the acetic acid solution, and also showed additional interactions of

chitosan with the three different polyols. The differences between the various samples were also visible in the XRD diffraction patterns. Crystallinity decreased when the polyol content increased, and was also dependent on the polyol type: crystallinity was the lowest with glycerol and the highest with sorbitol. Morphological observations were in accordance with the XRD conclusions. From SEM micrographs, a layered microstructure was observed embedded in a matrix phase. The polyol addition seemed to reduce the layered microstructure density. The crystallinity could be correlated to the rheological and mechanical properties: the sample with sorbitol exhibiting the highest properties and the sample with glycerol the lowest ones. The difference in results between glycerol and sorbitol may be explained by the possible sorbitol recrystallization at room temperature.

For the plasticized chitosan samples, tensile strength decreases when the polyol content increases while elongation at break increases with the polyol content. In addition, TGA results showed a slower thermal degradation for sorbitol formulations and faster for glycerol ones. Thermal degradation was also faster for chitosan samples containing a polyol as compared to the chitosan sample with only acetic acid (ChiA).

These results show that this plasticization technique is an interesting alternative to the traditional solution casting method to prepare chitosan films on a larger scale. Depending on the application considered (biomedical, packaging, agriculture, etc.), the plasticized chitosan formulation may be tailored according to requirements in terms of rheological, mechanical and physicochemical properties. A specific multiphase system could be appropriate for packaging when e.g., associated by melt-blending or co-extrusion with another thermoplastic polymer. Another system may be suited to produce fibrous permeable membranes for metal capture from wastewater, in order to take advantage of the good complexing ability of chitosan with metals. Finally, these materials may also be promising for tissue engineering applications to elaborate 2D or 3D scaffolds, considering the antibacterial activity of chitosan.

Acknowledgments

The authors gratefully acknowledge Ms. Verónica Martino of the BioTeam/LIPHT-ECPM research group in Strasbourg for her help with the first stage of this work. We also thank the following research associates at Polytechnique Montréal: Ms. Weawkamol Leelapornpisit for the TEM and SEM images, and Ms. Melina Hamdine for her assistance with the rheological measurements. Finally, the authors acknowledge the NIPMMP (Network for Innovative Plastic Materials and Manufacturing Processes) for the financial support of this work.

References

- Arvanitoyannis, I., Kolokuris, I., Nakayama, A., Yamamoto, N., & Aiba, S.-i. (1997). Physico-chemical studies of chitosan-poly(vinyl alcohol) blends plasticized with sorbitol and sucrose. *Carbohydrate Polymers*, 34(1–2), 9–19.
- Avérous, L. (2004). Biodegradable multiphase systems based on plasticized starch: A review. *Polymer Reviews*, 44(3), 231–274.
- Avérous, L., & Halley, P. J. (2009). Biocomposites based on plasticized starch. *Biofuels, Bioproducts and Biorefining*, 3(3), 329–343.
- Balau, L., Lisa, G., Popa, M., Tura, V., & Melnig, V. (2004). Physico-chemical properties of Chitosan films. *Central European Journal of Chemistry*, 2(4), 638–647.
- Brugnerotto, J., Lizardi, J., Goycoolea, F. M., Argüelles-Monal, W., Desbrières, J., & Rinaudo, M. (2001). An infrared investigation in relation with chitin and chitosan characterization. *Polymer*, 42(8), 3569–3580.
- Chen, S., Wu, G., & Zeng, H. (2005). Preparation of high antimicrobial activity thiourea chitosan-Ag⁺ complex. *Carbohydrate Polymers*, 60(1), 33–38.
- Domard, A., & Rinaudo, M. (1983). Preparation and characterization of fully deacetylated chitosan. *International Journal of Biological Macromolecules*, 5(1), 49–52.
- Dutta, P. K., Tripathi, S., Mehrotra, G. K., & Dutta, J. (2009). Perspectives for chitosan based antimicrobial films in food applications. *Food Chemistry*, 114(4), 1173–1182.

- Epure, V., Griffon, M., Pollet, E., & Avérous, L. (2011). Structure and properties of glycerol-plasticized chitosan obtained by mechanical kneading. *Carbohydrate Polymers*, 83(2), 947–952.
- Forsell, P. M., Hulleman, S. H. D., Myllärinen, A., Moates, P. J., Parker, G. K., & R. (1999). Ageing of rubbery thermoplastic barley and oat starches. *Carbohydrate Polymers*, 39(1), 43–51.
- Ilium, L. (1998). Chitosan and its use as a pharmaceutical excipient. *Pharmaceutical Research*, 15(9), 1326–1331.
- Kittur, F. S., Kumar, K. R., & Tharanathan, R. N. (1998). Functional packaging properties of chitosan films. *Zeitschrift für Lebensmitteluntersuchung und -Forschung A*, 206(1), 44–47.
- Kittur, F. S., Vishu Kumar, A. B., & Tharanathan, R. N. (2003). Low molecular weight chitosans – preparation by depolymerization with *Aspergillus niger* pectinase, and characterization. *Carbohydrate Research*, 338(12), 1283–1290.
- Kong, M., Chen, X. G., Liu, C. S., Liu, C. G., Meng, X. H., & Yu, L. J. (2008). Antibacterial mechanism of chitosan microspheres in a solid dispersing system against *E. coli*. *Colloids and Surfaces B: Biointerfaces*, 65(2), 197–202.
- Lavorgna, M., Piscitelli, F., Mangiacapra, P., & Buonocore, G. G. (2010). Study of the combined effect of both clay and glycerol plasticizer on the properties of chitosan films. *Carbohydrate Polymers*, 82(2), 291–298.
- Li, H., & Huneault, M. A. (2011). Comparison of sorbitol and glycerol as plasticizers for thermoplastic starch in TPS/PLA blends. *Journal of Applied Polymer Science*, 119(4), 2439–2448.
- Li, J., Zivanovic, S., Davidson, P. M., & Kit, K. (2011). Production and characterization of thick, thin and ultra-thin chitosan/PEO films. *Carbohydrate Polymers*, 83(2), 375–382.
- Manas-Zloczower, I., & Tadmor, Z. (2009). *Mixing and compounding of polymers: Theory and practice*. Cincinnati, OH, USA: Carl Hanser Verlag GmbH & Co. KG.
- Martino, V., Pollet, E., & Avérous, L. (2011). Novative biomaterials based on chitosan and poly(ϵ -caprolactone): Elaboration of porous structures. *Journal of Polymers and the Environment*, 19(4), 819–826.
- Mucha, M. (1998). Rheological properties of chitosan blends with poly(ethylene oxide) and poly(vinyl alcohol) in solution. *Reactive and Functional Polymers*, 38(1), 19–25.
- No, H. K., Young Park, N., Ho Lee, S., & Meyers, S. P. (2002). Antibacterial activity of chitosans and chitosan oligomers with different molecular weights. *International Journal of Food Microbiology*, 74(1–2), 65–72.
- Okuyama, K., Noguchi, K., Miyazawa, T., Yui, T., & Ogawa, K. (1997). Molecular and crystal structure of hydrated chitosan. *Macromolecules*, 30(19), 5849–5855.
- Osman, Z., & Arof, A. K. (2003). FTIR studies of chitosan acetate based polymer electrolytes. *Electrochimica Acta*, 48(8), 993–999.
- Pillai, C. K. S., Paul, W., & Sharma, C. P. (2009). Chitin and chitosan polymers: Chemistry, solubility and fiber formation. *Progress in Polymer Science*, 34(7), 641–678.
- Qi, L., Xu, Z., Jiang, X., Hu, C., & Zou, X. (2004). Preparation and antibacterial activity of chitosan nanoparticles. *Carbohydrate Research*, 339(16), 2693–2700.
- Qiao, X., Tang, Z., & Sun, K. (2011). Plasticization of corn starch by polyol mixtures. *Carbohydrate Polymers*, 83(2), 659–664.
- Quijada-Garrido, I., Laterza, B., Mazón-Arechederra, J. M., & Barrales-Rienda, J. M. (2006). Characteristic features of chitosan/glycerol blends dynamics. *Macromolecular Chemistry and Physics*, 207(19), 1742–1751.
- Ravi Kumar, M. N. V. (2000). A review of chitin and chitosan applications. *Reactive and Functional Polymers*, 46(1), 1–27.
- Rinaudo, M. (2006). Chitin and chitosan: Properties and applications. *Progress in Polymer Science*, 31(7), 603–632.
- Rivero, S., García, M. A., & Pinotti, A. (2010). Crosslinking capacity of tannic acid in plasticized chitosan films. *Carbohydrate Polymers*, 82(2), 270–276.
- Roberts, G. A. F. (1992). *Preparation of chitin and chitosan* (T.M.P. Ltd ed.). *Chitin chemistry*, pp 54–84.
- Rotta, J., Ozório, R. A., Kehrwald, A. M., de Oliveira Barra, G. M., de Melo Castanho Amboni, R. D., & Barreto, P. L. M. (2009). Parameters of color, transparency, water solubility, wettability and surface free energy of chitosan/hydroxypropylmethylcellulose (HPMC) films plasticized with sorbitol. *Materials Science and Engineering: C*, 29(2), 619–623.
- Sadeghi, A. M. M., Dorkoosh, F. A., Avadi, M. R., Saadat, P., Rafiee-Tehrani, M., & Junginger, H. E. (2008). Preparation, characterization and antibacterial activities of chitosan, N-trimethyl chitosan (TMC) and N-diethylmethyl chitosan (DEMC) nanoparticles loaded with insulin using both the ionotropic gelation and polyelectrolyte complexation methods. *International Journal of Pharmaceutics*, 355(1–2), 299–306.
- Shahidi, F., Arachchi, J. K. V., & Jeon, Y.-J. (1999). Food applications of chitin and chitosans. *Trends in Food Science and Technology*, 10(2), 37–51.
- Srinivasa, P. C., Ramesh, M. N., & Tharanathan, R. N. (2007). Effect of plasticizers and fatty acids on mechanical and permeability characteristics of chitosan films. *Food Hydrocolloids*, 21(7), 1113–1122.
- Takahashi, T., Imai, M., Suzuki, I., & Sawai, J. (2008). Growth inhibitory effect on bacteria of chitosan membranes regulated with deacetylation degree. *Biochemical Engineering Journal*, 40(3), 485–491.
- Talja, R. A., Helén, H., Roos, Y. H., & Jouppila, K. (2007). Effect of various polyols and polyol contents on physical and mechanical properties of potato starch-based films. *Carbohydrate Polymers*, 67(3), 288–295.
- Thirathumthavorn, D., & Charoenrein, S. (2007). Aging effects on sorbitol- and non-crystallizing sorbitol-plasticized tapioca starch films. *Starch – Stärke*, 59(10), 493–497.
- Valle, G. D., Buleon, A., Carreau, P. J., Lavoie, P.-A., & Vergnes, B. (1998). Relationship between structure and viscoelastic behavior of plasticized starch. *Journal of Rheology*, 42(3), 507–525.
- Van Soest, J. J. G., Hulleman, S. H. D., De Wit, D., & Vliegenthart, J. F. G. (1996). Changes in the mechanical properties of thermoplastic potato starch in relation with changes in B-type crystallinity. *Carbohydrate Polymers*, 29(3), 225–232.
- Van Soest, J. J. G., & Knooren, N. (1997). Influence of glycerol and water content on the structure and properties of extruded starch plastic sheets during aging. *Journal of Applied Polymer Science*, 64(7), 1411–1422.
- Wang, X., Du, Y., & Liu, H. (2004). Preparation, characterization and antimicrobial activity of chitosan–Zn complex. *Carbohydrate Polymers*, 56(1), 21–26.
- Yi, H., Wu, L.-Q., Bentley, W. E., Ghodssi, R., Rubloff, G. W., Culver, J. N., et al. (2005). Biofabrication with chitosan. *Biomacromolecules*, 6(6), 2881–2894.
- Zivanovic, S., Chi, S., & Draughon, A. F. (2005). Antimicrobial activity of chitosan films enriched with essential oils. *Journal of Food Science*, 70(1), M45–M51.
- Zivanovic, S., Li, J. J., Davidson, P. M., & Kit, K. (2008). Physical, mechanical, and antibacterial properties of chitosan/PEO blend films [correction]. *Biomacromolecules*, 9(4), 1355, 1355–1355.